

# InP/InGaAsP-Based Integrated 3-dB Trench Couplers for Ultra-Compact Coherent Receivers

Uppiliappan Krishnamachari, Sasa Ristic, Chin-Hui Chen, Leif Johansson, Anand Ramaswamy, Jonathan Klamkin, Erik Norberg, John E. Bowers, *Fellow, IEEE*, and Larry A. Coldren, *Fellow, IEEE*

**Abstract**—We present the design, fabrication, and test results for ultra-compact 3-dB frustrated total internal reflection-based trench couplers in an InP/InGaAsP monolithic integration platform. The trench coupler is integrated with phase modulators and a balanced photodiode (BPD) pair to enable a 180°-hybrid ultra-compact coherent receiver. Several trench splitter designs exhibit near 3-dB splitting with a loss of ~3 dB. The BPD pair is used to characterize coherent mixing of two input optical signals into the trench splitter, and coherence efficiency of 75% is achieved.

**Index Terms**—Beam splitter, coherent mixing, etched slot, frustrated total internal reflection (FTIR), 3-dB coupler, trench.

## I. INTRODUCTION

WAVEGUIDE couplers are important components in the realization of compact, integrated optical circuits due to their ability to split the light beam or change its direction in a short distance [1]. A compact optical mixing element is required to minimize the footprint and optical path length. The most commonly used beam splitter for photonic integrated circuits is the multimode interference (MMI) coupler, and although recent advances in MMI design have yielded lengths as short as 50  $\mu\text{m}$ , the devices are still limited in geometry due to radiation loss suffered in sharp bends [2]. In contrast, an etched trench that cuts the optical waveguide can perform 3-dB splitting within a submicrometer length. This is achieved by using the trench as a frustrated total internal reflection (FTIR) mirror, where the angle of the input waveguide incident on the trench is greater than the critical angle [3]. In a process analogous to quantum mechanical tunneling, the incident wave creates an evanescent field that penetrates into the lower index medium of the trench. If the gap width is small enough, this evanescent wave can couple across the gap to the waveguide on the other side and form the transmitted wave. The reflected wave still behaves as a totally internally reflected wave, exhibiting a small lateral Goos–Hanchen shift from the incident wave. The reflected and transmitted waves are complementary, behaving

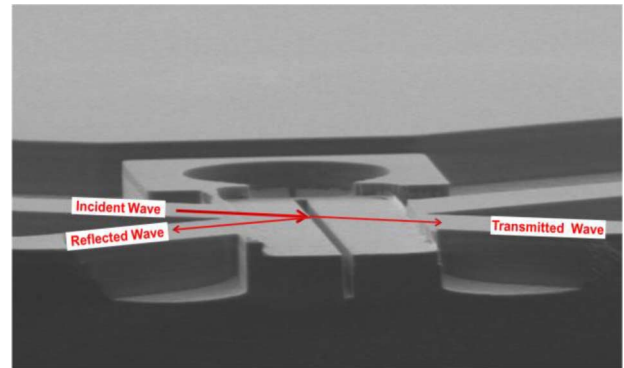


Fig. 1. SEM image of trench coupler illustrating reflection and transmission of a wave incident on the trench coupler.

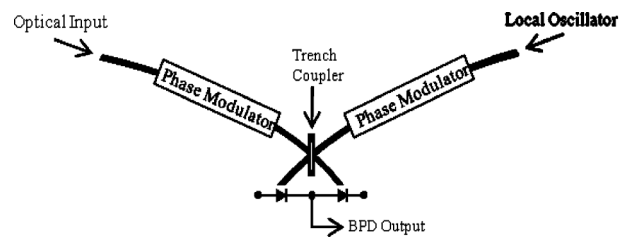


Fig. 2. Schematic of trench splitter-based coherent receiver.

as a 180° hybrid [4]. The splitting of the incident wave into reflected and transmitted signals is shown in Fig. 1.

The theoretical framework for an FTIR based 3-dB coupler design has been explained elsewhere [5]. Demonstration of FTIR trench beam splitters has been reported in both AlGaAs and InGaAsP material systems [6], [7]. In this letter we present a coherent receiver structure with a trench beam splitter integrated with phase modulators and a balanced uni-traveling-carrier photodiode (UTC-PD) for use in an ultra-compact coherent optical receiver with feedback [8]. A schematic of the coherent receiver can be seen in Fig. 2.

## II. DESIGN AND SIMULATION

In this design, we use benzocyclobutene (BCB) with a refractive index of 1.57 to fill the trench. With a calculated effective index of 3.265 for the InGaAsP optical waveguide, the critical angle for the semiconductor/BCB interface is 28.5°. We fabricated waveguides with values of crossing angle,  $\theta$ , that range from 27°–32° to account for any error in the index of the semiconductor or the BCB. Two-dimensional finite-difference time-domain (FDTD) simulations were carried out for each of these angles in order to find the gap width corresponding to

Manuscript received August 30, 2010; revised October 27, 2010; accepted November 27, 2010. Date of publication December 17, 2010; date of current version February 24, 2011.

The authors are with the University of California, Santa Barbara Engineering Science Building, Electrical and Computer Engineering, Santa Barbara, CA 93106-9560 USA (e-mail: ukrishna@ece.ucsb.edu; ristic@ece.ucsb.edu; janet@ece.ucsb.edu; leif@ece.ucsb.edu; anand@ece.ucsb.edu; klamkin@engineering.ucsb.edu; norberg@ece.ucsb.edu; bowers@ece.ucsb.edu; coldren@ece.ucsb.edu).

Color versions of one or more of the figures in this letter are available online at <http://ieeexplore.ieee.org>.

Digital Object Identifier 10.1109/LPT.2010.2100376

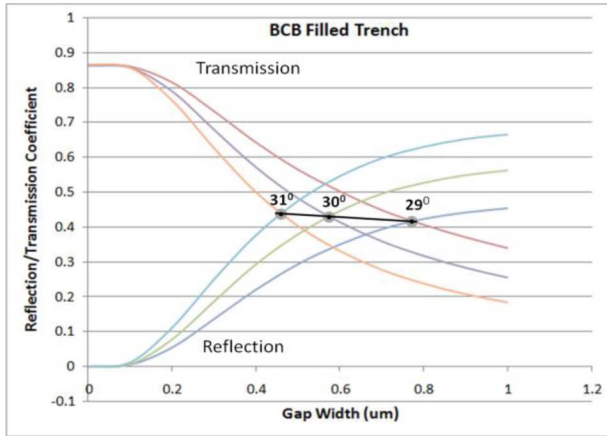


Fig. 3. Two-dimensional FDTD simulations of trench coupler splitting for TE polarized light.

3-dB splitting. There are many assumptions in using a two dimensional structure for numerical simulation. For one, we assume that the trench etch is deep enough to encompass the optical mode. In practice, the aspect ratio of the etch is limited. More importantly, the 2-D simulations significantly underestimate loss and do not take into account beam divergence due to nonidealities of fabrication such as tilted sidewalls, which is a significant problem in high aspect ratio etching [9]. However, we can still see many trends that help guide the design.

Simulated reflection and transmission of transverse electric (TE) polarized light for different trench widths are shown in Fig. 3. For ease of interpretation, only crossing angles  $29^\circ$ ,  $30^\circ$ , and  $31^\circ$  are shown. The point where the reflection and transmission curves intersect is the 3-dB splitting point. The trend from these simulations is that the design width decreases as the crossing angle is increased above the critical angle. The simulated widths for angles  $29^\circ$ – $31^\circ$  were found to be in the range of  $0.4\ \mu\text{m}$ – $0.8\ \mu\text{m}$ . However, considering that 2-D simulations overestimate the trench width needed for 3-dB splitting [6], we select a width range of  $0.15\ \mu\text{m}$ – $0.55\ \mu\text{m}$  for our crossing angle range of  $27^\circ$ – $32^\circ$ . Simulations for transverse magnetic (TM) polarization yield a 3-dB gap width of less than  $0.1\ \mu\text{m}$ . Because this is impractically small for fabrication, we design 3-dB splitters for TE polarized light.

The device epitaxial structure has roughly  $1.8\ \mu\text{m}$  of p-InP cladding on top of  $0.4\ \mu\text{m}$  of an InGaAsP multiple quantum well (MQW) optical waveguide core. The optical waveguide consists of a multiple quantum well (MQW) stack of 15 compressively strained wells and 16 tensile strained barriers. The QW width is  $65\ \text{\AA}$  and the barrier width is  $80\ \text{\AA}$ .

Ideally, the etch depth should be below the MQW core and have smooth and vertical sidewalls. We aim for a target etch depth of  $3.2\ \mu\text{m}$  which corresponds to an aspect ratio of larger than 10:1 for our design widths, presenting a serious challenge in realizing a straight sidewall trench of sufficient depth. In high aspect ratio etching, an RIE-lag effect limits the etch rate of small features with greater than 10:1 aspect ratios [10]. However, simulations show that we can etch a wider area around the trench by as much as  $1\ \mu\text{m}$  without causing significant reflection of the mode at the etched interface. Pre-etching of the

trench area prior to the actual trench etch can reduce our target etch depth to  $\sim 2.2\ \mu\text{m}$ , bringing the aspect ratio of most of our design widths down to 7:1.

### III. FABRICATION

In order to fabricate the coherent receiver, integrated UTC-PDs are first defined by selective removal of photodiode layers in nondetector regions. Waveguides are deeply etched to a depth of  $\sim 3\ \mu\text{m}$  using  $\text{Cl}_2 : \text{H}_2 : \text{Ar} = 7.6 : 11.4 : 2\ \text{sccm}$ , 800 W ICP power, 125 W RIE power,  $p = 8\ \text{mT}$  and  $t = 120\ \text{s}$ . Contact metal is deposited and high energy Helium implants are used to electrically isolate the PDs in the balanced photodiode pair. As mentioned above, windows over the trench areas are opened and pre-etched by  $\sim 0.8\ \mu\text{m}$ . Topography of the waveguide is planarized using reflowed polymethylglutarimide (PMGI) with openings over the pre-etched window in order to write the trench features using electron beam lithography.

The trench etch was carried out on an inductively coupled plasma—reactive ion etching (ICP-RIE) system employing  $\text{Cl}_2/\text{H}_2/\text{Ar}$  chemistry.  $\text{Cl}_2$  is generally known to contribute to chemical etching while Ar acts as a physical milling process. The addition of  $\text{H}_2$  acts to balance these two processes [11]. As a starting point, we used the chemistry of the waveguide etch. To find optimal etch conditions for a deep trench, we varied etch time, pressure, RIE and ICP powers, and the relative flows of  $\text{Cl}_2$ ,  $\text{H}_2$  and Ar. The optimized trench etch condition was  $\text{Cl}_2 : \text{H}_2 : \text{Ar} :: 7 : 12 : 8\ \text{sccm}$ , 250 W RIE power, 800 W ICP power,  $p = 8\ \text{mT}$ ,  $t = 350\ \text{s}$ , which is very close to the waveguide etch process except for an increased Ar flow and much longer etch time. The Ar presumably continues physical milling of the trench even after the trench gets too deep for  $\text{Cl}_2$  chemical etching to occur, thus achieving the necessary sidewall straightness. The longer etch time is necessitated by the RIE lag effect and requires a very thick dielectric mask of  $\sim 6000\ \text{\AA}$   $\text{SiO}_2$  to withstand the etch to  $\sim 2.5\ \mu\text{m}$  depth. After etching, BCB 4022-35 is used to fill the trench features. Thick pad metal is deposited for the metal traces, and lastly the devices are thinned and cleaved for characterization.

### IV. TRENCH COUPLER CHARACTERIZATION

Trench devices were tested for splitting ratio and loss using a laser source emitting at  $1548.5\ \text{nm}$  with 10 dBm at the facet. Splitting ratio was determined simply by taking the detected photocurrent in a given detector over the sum of the photocurrent in both detectors. The trench loss was determined by comparing current in one input modulator with the total current in the detectors. First, current in a modulator is measured at high reverse bias voltage so that the modulator absorbs practically all input light. Assuming modulator responsivity to be 100% under this condition, the measured modulator photocurrent represents the optical power at the input of the modulator. Second, the total current in the two detectors is measured for an unbiased input modulator. Assuming a detector responsivity of 100%, the measured detector photocurrent represents the total optical power at the input of the photodetectors. Dividing the modulator current over the total detector current represents the optical power lost in the trench, overestimated by the fraction of optical power lost in the modulator due to scattering, free-carrier absorption, and

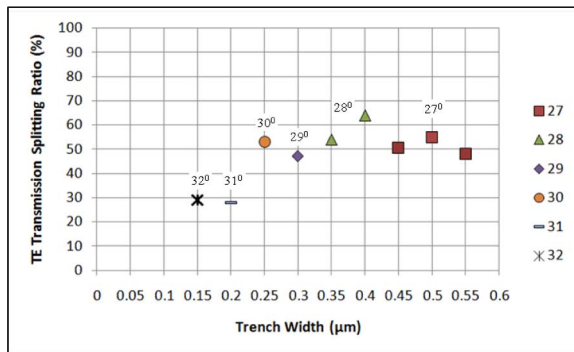


Fig. 4. TE splitting ratios of several crossing angles.

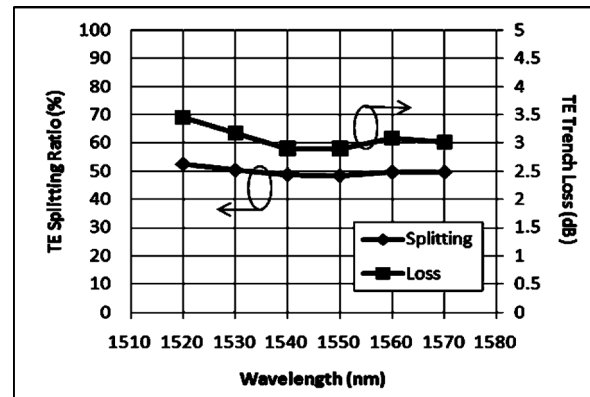


Fig. 5. Wavelength insensitivity of TE splitting ratio and loss.

other mechanisms that do not contribute to photocurrent. The maximum power transmitted through the trench occurs for TE polarized light, which also corresponds to the optimized splitting ratio for these devices. TM polarized light typically had a very low transmission and very high reflection, which is in agreement with simulations. Optical loss of an unbiased modulator is measured to be 2 dB/mm by comparing devices with 300  $\mu\text{m}$  and 500  $\mu\text{m}$  modulator lengths. Subtracting this from the measured loss using the above method, trench coupler losses for TE polarized light fell in the range of 2.5–3.5 dB, which is very close to the AlGaAs trench coupler losses reported in [6].

Many device designs throughout the range of crossing angles (and corresponding trench widths) exhibited  $\sim 50 : 50$  splitting for TE polarized light. Fig. 4 shows several devices that achieved 3-dB splitting at different crossing angles/trench widths. The crossing angles  $31^\circ$  and  $32^\circ$  did not achieve 3-dB splitting most likely because the RIE-lag effect limited the etch depth of the corresponding small trench widths. For trench widths greater than 200 nm, the trench depth seems to have been large enough to extend over most of the optical mode, and the crossing angles of  $27^\circ$ – $30^\circ$  achieved  $\sim 3$ -dB splitting. The measured values cannot be directly correlated to the 2-D FDTD simulations, but the trend of smaller 3-dB trench width for higher crossing angles is clearly observed. The trench couplers were tested with a Tunics tunable external cavity laser source over the  $C$ -band wavelength range. Splitting and loss for both polarizations are seen to be relatively wavelength insensitive. The wavelength dependence of the TE transmission splitting ratio and trench loss are plotted in Fig. 5.

Lastly, the integrated BPD pair was used to observe the coherence efficiency of the coupler. A signal was split in two and input into both sides of the coherent receiver, with one of the arms being phase modulated. The envelope of the balanced signal corresponds to the constructive and destructive mixing of the two signals. Comparing this envelope to the maximum envelope theoretically obtainable for the detected photocurrent levels [12], we observed a coherence efficiency of 75%. We suspect that the coherence efficiency suffers penalties due to modal and polarization mismatch between the two arms of the interferometer.

## V. CONCLUSION

We have designed, fabricated, and characterized 3-dB FTIR-based trench couplers. Splitting ratio is optimized for TE polarization and shows little wavelength dependence over the  $C$ -band. The small footprint of the 3-dB trench couplers makes them an enabling technology for ultra-compact InP PICs.

## REFERENCES

- [1] Y. Chung, R. Spickermann, B. Young, and N. Dagli, "A low loss beam splitter with an optimized waveguide structure," in *Digest on LEOS 1992 Summer Topical Meeting*, 1992, pp. B61–B62.
- [2] Y. Ma, S. Park, L. Wang, and S. T. Ho, "Ultra-compact multimode interference 3-dB coupler with strong lateral confinement by deep dry etching," *IEEE Photon. Technol. Lett.*, vol. 12, no. 5, pp. 492–494, May 2000.
- [3] I. Court and F. von Willisen, "Frustrated total internal reflection and application of its principle to laser cavity design," *Appl. Opt.*, vol. 3, pp. 719–726, 1964.
- [4] M. Daehler and P. A. R. Ade, "Michelson interferometer with frustrated-total-internal-reflection beam splitter," *J. Opt. Soc. Amer.*, vol. 65, pp. 124–130, 1975.
- [5] N. Huntoon, M. Christensen, D. MacFarlane, G. Evans, and C. S. Yeh, "Integrated photonic coupler based on frustrated total internal reflection," *Appl. Opt.*, vol. 47, pp. 5682–5690, 2008.
- [6] B. Kim, Y. Chang, and N. Dagli, "Compact etched beam splitters in weakly guiding GaAs/AlGaAs waveguides," in *Proc. Integrated Photonics and Nanophotonics Research and Applications*, 2009, OSA Technical Digest, Optical Society of America.
- [7] E. J. Norberg, J. S. Parker, U. Krishnamachari, R. S. Guzzon, and L. A. Coldren, "InGaAsP/InP based flattened ring resonators with etched beam splitters," in *Proc. IPNRA, IWAI*, Honolulu, HI, 2009.
- [8] H. F. Chou, A. Ramaswamy, D. Zibar, L. A. Johansson, J. E. Bowers, M. Rodwell, and L. A. Coldren, "High-linearity coherent receiver with feedback," *IEEE Photon. Technol. Lett.*, vol. 19, no. 12, pp. 940–942, Jun. 15, 2007.
- [9] B. Kim and N. Dagli, "Submicron etched beam splitters based on total internal reflection in GaAs–AlGaAs waveguides," *J. Lightw. Technol.*, vol. 28, no. 13, pp. 1938–1943, Jul. 1, 2010.
- [10] R. Gottscho, C. W. Jurgensen, and D. J. Vitkavage, "Microscopic uniformity in plasma etching," *J. Vac. Sci. Technol. B*, vol. 10, pp. 2133–2133, 1992.
- [11] S. L. Rommel *et al.*, "Effect of H<sub>2</sub> on the etch profile of InP/InGaAsP alloys in Cl<sub>2</sub>/Ar/H<sub>2</sub> inductively-coupled-plasma reactive ion etching chemistries for photonic device fabrication," *J. Vac. Sci. and Technol. B*, vol. 20, pp. 1327–1330, 2002.
- [12] P. Y. Painchaud, M. Poulin, M. Morin, and M. Têtu, "Performance of balanced detection in a coherent receiver," *Opt. Express*, vol. 17, pp. 3659–3672, 2009.